

# Effect of Silymarin and/or Bone Marrow-Derived Mesenchymal Stem Cells on Carbon Tetrachloride-Induced Hepatotoxicity in Rats

Tariq I Almundarij<sup>1\*</sup>, Abdel Kader A Zaki<sup>1,2</sup>, Yousef M. Alharbi<sup>1</sup>, Saleh M. Albarrak<sup>1</sup>, Tamim S Alqarawi<sup>1</sup> and Faten A M Abo-Aziza<sup>3\*</sup>

<sup>1</sup>Department of Veterinary Medicine, College of Agriculture and Veterinary Medicine, Qassim University, Buraydah, Saudi Arabia

<sup>2</sup>Department of Physiology, Faculty of Veterinary Medicine, Cairo University, Giza, Egypt

<sup>3</sup>Department of Parasitology and Animal Diseases, Veterinary Research Division, National Research Centre, Cairo, Egypt

\*Corresponding Authors: Faten A M Abo-Aziza ([faten.aboaziza@gmail.com](mailto:faten.aboaziza@gmail.com))  
Tariq I Almundarij ([tmndri@qu.edu.sa](mailto:tmndri@qu.edu.sa))

## ABSTRACT

Hepatic fibrosis has been diagnosed in more than 10% of the world population and is still with limited treatments. This work explored whether silymarin and bone marrow-derived mesenchymal stem cells (BM-MSCs) combination can remodel the hepatotoxicity induced by carbon tetrachloride (CCl<sub>4</sub>) in rats. Fifty rats were equally distributed into five groups: healthy control, CCl<sub>4</sub> hepatotoxicity rat model, CCl<sub>4</sub> + silymarin treated, CCl<sub>4</sub> + BM-MSCs treated, CCl<sub>4</sub> + silymarin + BM-MSCs treated. Serum liver function tests, hepatic tissue oxidative enzymes and cytokines were assessed. Akt and P-Akt proteins expression was estimated by Western blot. Livers were examined histologically using two types of staining. The cultured BM-MSCs positively expressed CD73, CD105, and CD29 and negatively expressed CD34 and CD45. The morphology of the BM-MSCs changed from spindle-shaped to oblate-shaped after hepatogenic differentiation. In CCl<sub>4</sub> hepatotoxicity rat model, a significant increase in transaminases ( $P < 0.01$ ), bilirubin ( $P < 0.05$ ), malondialdehyde, and TNF- $\alpha$  ( $P < 0.01$ ) was observed. There was a noticeable drop in the catalase ( $P < 0.01$ ), superoxide dismutase, glutathione peroxidase, interleukins (IL) -4, -10, and -17 ( $P < 0.05$ ). A marked elevated IL-17 and reduced TNF- $\alpha$  levels were noticed in the rats treated with silymarin ( $P < 0.05$ ). Treatment with BM-MSCs or the combination of silymarin and BM-MSCs restored the cytokine levels and ameliorated all the hepatic bio indices to normal levels. According to the obtained results, a combination of BM-MSCs and silymarin could alleviate liver hepatotoxicity. Furthermore, the results were supported by the Akt/p-Akt signaling cascade via down-regulation of Akt phosphorylation.

**Keywords:** Bone marrow-derived mesenchymal stem cells, Carbon tetrachloride, Hepatotoxicity, Rat, Silymarin

## Correspondence:

Faten A M Abo-Aziza

Department of Parasitology and Animal Diseases, Veterinary Research Division, National Research Centre, Cairo, Egypt

Email: [faten.aboaziza@gmail.com](mailto:faten.aboaziza@gmail.com)

Tariq I Almundarij

Department of Veterinary Medicine, College of Agriculture and Veterinary Medicine, Qassim University, Buraydah, Saudi Arabia

Email: [tmndri@qu.edu.sa](mailto:tmndri@qu.edu.sa)

## INTRODUCTION

Liver disease is a broad term that covers all the potential problems that inhibit the liver from performing its designated functions. The main responsibility of the liver is to detoxify the majority of drugs and toxins and get rid of them outside the body. However, some of these toxins can cause liver injury, which is termed hepatotoxicity. Furthermore, the general liver complaint in many countries is the fatty liver disease, which is the accumulation of excess fat in the liver cells [1]. Nonalcoholic Fatty Liver Disease (NAFLD) is considered one of the most primary causes of cirrhosis. Fibrosis of the liver is a huge problem that leads to organ dysfunction [2]. Hepatic fibrosis has been diagnosed in more than 10% of the world population and is still a main common health disease with limited treatment options and a variety of underlying etiologies [3]. Fibrosis is typically accompanied by the proliferation of hepatic parenchymal cells in the early stage as well as by interchanging mediators and cells. A number of issues arise when the liver is diagnosed with fibrosis, which follows the pathological process of chronic disease that begins with the damage and ends with the healing process, matrix protein deposition, and remodeling. It is accompanied by loss of both endothelium and parenchyma with macrophage stimulation and inflammatory cues [4]. Hepatic stellate cells (HSCs) have been documented to induce and form fibrosis through a membranous signals cascade as PI3K/Akt/mTOR [5]. These signals are responsible for cell cycles and

differentiation [3]. Prevalence of 7 – 10% NAFLD has been reported in Saudi Arabia [6]. The main risk factors that are very popular in Saudi Arabia are diabetes mellitus, hyperlipidemia as well as obesity, with some records suggesting 23.7%, 54% and 35.5% prevalence respectively [7]. The most recent WHO data released in 2017 recorded 1,995 liver disease deaths in Saudi Arabia which is 2.05% of total deaths. The age depending mortality rate was 13.33 from each 100,000 population and Saudi Arabia was ranked as #99 in the world for liver disease [8].

Scientists face several problems when dealing with the abovementioned damage to liver tissue, notwithstanding the myriad of the used therapy to prohibit complications and slope the progression rate. Although liver transplantation is widely considered an effective solution; Its implementation is limited due to the high costs, donor's scarcity and rejection of the transplanted organ [9]. Liver cells transplantation can play an alternative technique to ameliorate liver regeneration. Nonetheless, there is a deficiency in superior *in vitro* primary hepatocytes. They are difficult to propagate and their hepatic characteristics are easily lost [10]. Significant evidence shown in past studies suggests that treatment by silymarin can improve acute and chronic hepatic diseases [11]. Silymarin is a natural complex derived from the common plant (*Silybum marianum*). The activity of silymarin includes the augmentation of hepatic glutathione and stimulation of *RNA polymerase I* activity, in addition to its contribution to

the hepatic antioxidant protection [12]. The hepatoprotective and antioxidant activity of silymarin inhibits the free radicals produced from the metabolism of toxic materials such as CCl<sub>4</sub> and ethanol [12]. In the case of liver fibrosis, silymarin has an anti-fibrotic effect during signal transduction and also inhibits protein kinases. In addition, it may interact with intracellular signaling pathways [13].

There is a need for additional support to control liver damage. In recent years, mesenchymal stem cells (MSCs) have been studied extensively. Their dual characteristics of continuous own-renewal and the ability to differentiate into a variety of mature tissue types favor their use in regenerative medicine [15]. These MSCs are adult stem cells found in numerous tissues, including bone marrow and the umbilical cord, that have the ability to give rise to diverse cell types in the laboratory, such as cartilage, bone, fat, tendon, ligament, and muscle cells. Numerous studies have established the positive effects of MSCs on the regeneration of damaged tissue, reduction of inflammation and oxidative stress, and modulation of immune reactions [15]. These MSCs can be separated from numerous tissues (e.g., adipose tissue, bone marrow, amniotic fluid, menstrual blood, the umbilical cord tissue and blood) and purified. Thus, because of the shortage of sources for the transplantation of liver or hepatocyte, mesenchymal stromal cell therapy is being seen as an effective novel approach for the repair of liver damage [1]. In the current study, a CCl<sub>4</sub>-induced hepatotoxicity rat model was created because of the close similarity to fibrosis or even cirrhosis in humans [16][56]. Although the anti-inflammatory, antioxidant and antiapoptotic effects of standard drug silymarin and MSCs-based therapy have been reported, the possibility of combining these treatments to repair hepatotoxicity has not yet been evaluated or discussed in detail. Therefore, in the present work, we hypothesized that a combination of the two treatments might augment the outcome when compared to the administration of each treatment separately. The factors evaluated in the study included liver enzyme and antioxidant activity, liver cellular architecture, Akt/p-Akt protein expression, and cytokine levels.

## MATERIALS AND METHODS

### *Ethical standard*

The current work was permitted through the Animal Ethics Committee of Qassim University (QU) (No. 3432). The experiments were consistent with the guides recognized by the International Animal Ethics Committee and were carried out according to local laws and regulations.

### *Animals*

A total of fifty healthy male Wistar albino rats (150 - 180 g) were transported from the King Saud University laboratory center in Riyadh to suitable housing under hygienic conditions at the Department of Veterinary Medicine of the QU Faculty of Agriculture and Veterinary Medicine in Buraydah, Saudi Arabia. The animals were kept in cages (30 × 35 × 15 cm per 4-5 rats). All animals received a commercial diet formulated to supply all the recommended nutrients [17]. Feed and water were provided *ad libitum*. Animals care was permitted by the QU Animal Ethics Committee and was monitored throughout the experimental duration.

### *CCl<sub>4</sub>-induced hepatotoxicity rat model*

The CCl<sub>4</sub>-induced rat model is mostly considered as the typical and commonly used of the various liver hepatotoxicity models (4). In the present work, the rat model was implemented via intraperitoneal (i.p.) injection (1.0 mg/kg) of diluted CCl<sub>4</sub> (BDH Chemicals, England) in olive oil (1:1.5, vol/vol) twice a week for 70 days.

### *Bone marrow-mesenchymal stem cells (BM-MSCs)*

Five 50-day-old albino Wistar rats were used for isolation of MSCs from BM of the femur and tibia as described previously, with some modification [18]. Briefly, the rats were killed using sodium pentobarbital anesthesia and the bones excised. The BM was harvested by inserting a syringe containing complete conditioned DMEM warmed medium with glucose (1 g/L) + fetal bovine serum (10%) into the bone and extracting the medium with the red marrow, which was collected in Petri dishes (100 mm) contain one mL heparin (2000 IU / 0.2 mL). The suspension was centrifuged twice with phosphate buffer saline (PBS) to discard all remaining tissues. After that, alpha minimum essential medium (α-MEM) was added, and the diluted BM was used with similar amount of sodium carbonate buffer solution (0.1%) for lysis of the red blood cells as described previously [19]. The mononuclear cells (MNCs) were isolated and grown as previously mentioned [20]. Briefly, the cells were incubated with 5% CO<sub>2</sub> for 24 h, at 37 °C to adhere, and non-adherent were washed out once the medium was changed. Maintenance of the attached cells was carried out with α-MEM complemented with fetal bovine serum (20%), 55 μM 2- mercaptoethanol, 2 mM L-glutamine and 2 kinds of antibiotics. Culture dishes were preserved in a humid incubator with 5% CO<sub>2</sub> at 37 °C. The medium was regularly changed every 2 days. When the attached cells of the 1st culture had achieved 80 % confluence, sub-culturing was done and named passage zero. The following passages were numbered accordingly. Adherent cells of the primary cell culture were released by sterile trypsin-EDTA solution (0.25%) at 37 °C after a double wash with PBS. Additional fetal bovine serum (100 μL) was used to for trypsin inactivation. The cells were pelleted after centrifugation at low speed followed by division into two parts via the same means. Each part was plated to increase the cell number. All the previous procedures were performed using sterile instruments under aseptic conditions in a laminar flow safety cabinet with filtered air.

### *Immunophenotype analysis of BM-MSCs*

Immunophenotype analysis was performed by the detection of cell surface markers using flow cytometry [21]. All major markers for MSCs cell surface as CD45, CD34, CD73, CD29, and CD105 were evaluated by FACS Calibur flow cytometer (BD Bioscience, San Jose, CA, USA). A count of 0.2 × 10<sup>6</sup> cells was washed twice using PBS together with 1% bovine serum albumin (Sigma-Aldrich, USA) then stained with anti-CD34, anti-CD45, anti-CD73, anti-CD29, and anti-CD105 antibodies (BD Biosciences). An isotype was used as control.

### *Viability % and proliferation capability of BM-MSCs*

Trypan blue stain was used to evaluate the viability of the BM-MSCs with the exclusion of the dead cells [22]. The proliferation of the confluent BM-MSCs (80%) was evaluated using a bromodeoxyuridine (Brd-U) integration assay kit (Invitrogen). Cells were seeded for 2-3 days at a density of 1 × 10<sup>4</sup> / well on two-well chamber slides (Nunc) and then incubated one day with diluted BrdU solution followed by staining. The positive-stained and total cells number were counted along ten successive images. The proliferation capacity of the BM-MSCs was

measured by way of positive BrdU cells percentage over the total number of nucleated cells [23]. An indirect manner was used for the determination of mitochondrial enzymes activity by applying dimethylthiazol-diphenyltetrazolium bromide (MTT) assay. The cells were subjected to 1 h incubation in 96-well plates among 0.2 mg MTT / mL medium, at 37 °C to produce formazan following reduction. After that, the solution was discarded, and 0.04 N HCl / 1 mL isopropanol was added to solubilize the formazan. After shaking for 5 min, formazan quantity was then calorimetrically evaluated at 570 nm wavelength (Guan *et al.*, 2011).

#### **Hepatogenic differentiation of BM-MSCs**

Induction of hepatogenic differentiated cells was carried out in three steps (conditioning, differentiation, and maturation) according to the method of Ye *et al.* [24]. The BM-MSCs at the 3<sup>rd</sup> passage a density of  $5 \times 10^3$  were cultured on collagen type I-coated flasks (Falcon) with a growth medium until confluency. Twenty-four h later, the cells were pre-cultured in a serum free Iscove's Modified Dulbecco's Medium (IMDM, Gibco, USA) complemented by 20 ng/mL epidermal growth factor (EGF, ITSI-Biosciences, USA) and 10 ng/mL basic fibroblast growth factor (bFGF2, ITSI-Biosciences, USA) for two days (conditioning step). For cell differentiation step induction, cells were incubated in IMDM including 20 ng/mL hepatocyte growth factor (HGF, ITSI-Biosciences, USA), 10 ng/mL bFGF2, and 0.61g/L nicotinamide (Lonza, Switzerland) for seven days. To induce maturation step, the cells were incubated up to 21 days among IMDM complemented with 20 ng/mL HGF, 20 ng/mL oncostatin M (OMS, ITSI-Biosciences, USA), 1  $\mu$ M/L dexamethasone (Dex, Sigma-Aldrich, USA), and 50 mg/mL insulin transferrin selenium (ITS, Lonza, Switzerland). For steps 2 and 3, the medium was changed twice weekly. The differentiated cells were then assessed morphologically at different time points: at the end of the differentiation step (Day 7), midway (Day 14) and at the termination of maturation step (Day 21).

#### **Injection of BM-MSCs**

After xylazine (10 mg/kg) anesthesia, intravenous (i.v.) injection was used as the route of administration in the rats. Prior to injection, xylol was used to wash the tail and to render the four tail veins more prominent. A suspension ( $5 \times 10^5$  cells in 50  $\mu$ L PBS) was prepared and injected slowly into two tail veins. After injection, using cotton balls, a gentle pressure was applied at the site of injection to prevent later draining and leakage of the cell suspensions.

#### **Experimental design**

The rats were randomly equally distributed (ten rats / group) as follows: (1) the apparently healthy control group that was i.p. injected with olive oil 2 times / week for 70 days; (2) the CCl<sub>4</sub>-induced hepatotoxicity rat model group that injected with CCl<sub>4</sub> 2 times / week for 70 days; (3) the CCl<sub>4</sub> + silymarin group received 25 mg/kg silymarin (Sedico Pharmaceutical Co., Cairo, Egypt) via orogastric tube as previously described (Abdel-Salam *et al.* 2012) once a day for 70 days; (4) the CCl<sub>4</sub> + BM-MSC group that on the day 60 and day 70 received a dose of  $5 \times 10^5$  BM-MSCs through the tail veins; (5) the CCl<sub>4</sub> + BM-MSC + silymarin group treated via the same regimen as groups 2,3, and 4. On Day 80, animals were sacrificed, blood samples and livers were collected and divided into two parts. One part was immediately stored at -80 °C in liquid nitrogen for homogenization and biochemical analysis, and the other part was stained using Masson's trichrome (MTC) and hematoxylin and eosin (H&E). The sera were

obtained from the blood samples and then deactivated at 56 °C for 30 min for the nonspecific agglutinins removal or inactivate complement proteins, and the samples were stored at -20 °C until used.

#### **Liver function parameters**

Following instructions in the enclosed pamphlets, commercially available kits (BioMerieux, SA) were used to calorimetrically estimate the levels of the serum protein profile (total protein and albumin) and liver-associated enzymes involving alanine aminotransferase (ALT), aspartate aminotransferase (AST), alkaline phosphatase (ALP) and the hepatocellular markers of total bilirubin (T. Bili) and direct bilirubin (D. Bili). The globulin level was also calculated.

#### **Antioxidant activity**

Specimens of the dissected livers were weighed and homogenized in PBS (pH 7.4) to give a 20% (w/v) homogenate, followed by sonication at low speed [25]. Ten min. centrifugation was done at 10,000 r.p.m and 4 °C and the supernatants were taken for malondialdehyde (MDA) determination to present the hepatic lipid peroxide formation. Further dilution of the supernatants to 2% was carried out with PBS to determine hepatic glutathione peroxidase (GPx), catalase (CAT), and superoxide dismutase (SOD) enzymes activities using SPECTRUM kits (BioMerieux Ltd, UK). Absorbencies were measured spectrophotometrically at 450 nm, 340 nm, 560 nm, and 520 nm, respectively.

#### **Cytokine profiles**

ELISA kits (Assaypro, USA) were used to perform the assay of the levels of cytokines (TNF- $\alpha$ , IL-4, IL-10, and IL-17) in the collected sera, and the color change was measured by microplate ELISA reader (Dynatic product, USA) at 450 nm according to the manufacturer's instructions.

#### **Western blot analysis**

Three equal pieces of liver tissue were dissected from each group and homogenized separately over ice in lysis buffer for 30 min, followed by a cooling centrifugation for 10 min at 12,000 r.p.m to clarify the lysate. The supernatants were then collected and kept at -80 °C to be used. Protein concentrations were commercially determined by available kits (BioMerieux, SA). Identical portions were subsequently run or electrophoresed on 10% SDS-polyacrylamide gel. Proteins were relocated on nitrocellulose membranes following by blocking using 5% skim milk in 1  $\times$  Tris-buffered saline/Tween 20 (TBST) for 2 h and incubated overnight with primary antibodies against Akt (1:1000) and p-Akt (1:2000) (Sigma-Aldrich, USA). The membranes were washed and incubated with horseradish peroxidase-conjugated goat anti-rabbit or anti-mouse IgG (PharMingen).  $\beta$ -actin was applied on the same membrane as the loading control and then bands immunoreactivity were visualized using chemiluminescence. The intensities of the bands were analyzed quantitatively by means of IMAGEJ software and relatively normalized and calculated to the correlated control  $\beta$ -actin [26].

#### **Histopathological studies**

Immediately after the experiment ended, the livers were preserved in neutral buffered formalin solution (10%). The fixed specimens were treated via the conservative paraffin-embedding technique, ethanol dehydration, xylene cleaning, and melted paraffin wax embedding inside an incubator adjusted at 60 °C. Paraffin blocks were obtained to get sections of 4  $\mu$ m thick followed by H & E staining. Another section from the same paraffin block was stained with Masson's trichrome staining (MTC) to

confirm and evaluate the fibrosis degree, and also to detect any hidden minor proliferative fibrous reaction that might have failed to be taken up by the H & E inspection [27]. All sections were examined microscopically and photographed.

#### Statistical analysis

The results were calculated and statistically analyzed via the Windows SPSS version 19 software. One-way analysis of variance (ANOVA) was used to identify differences between groups. In the status of significant differences, the Student-Newman-Kuels test was performed. All data were recorded on an individual basis. Duncan's New Multiple Range test was applied to determine significant differences ( $P < 0.05$  and  $P < 0.01$ ). Data were stated as means  $\pm$  standard error (SE).

## RESULTS

The BM-MSCs were isolated from the rat BM. The cells were cultured to adhere on five culture dishes. The cells were regularly observed via inverted microscope and they continued to multiply to reach 80% confluence after 14 days (Figure 1A). Serial passages were performed, and the viability and cell proliferation were assayed at the 3<sup>rd</sup> passage, with Trypan blue examination showing cell viability of  $95.54 \pm 3.22\%$ . Proliferation was evaluated by BrdU incorporation assay. The percentage of BrdU positive cells with brown-stained nuclei was 75.12 (Figure 1C). The proliferation was indicated by the OD of the formazan measurement in cells at 80% confluence. The released formazan was  $0.111 \pm 0.08$ . Phenotypic analysis showed that the cultured BM-MSCs positively expressed CD73 (91.13%), CD105 (89.51%), and CD29 (88.75%), while they negatively expressed CD34 and CD45 antibody staining. The untreated control sample exhibited 0.21% +ve population and 99.79% -ve population (Figure 2).

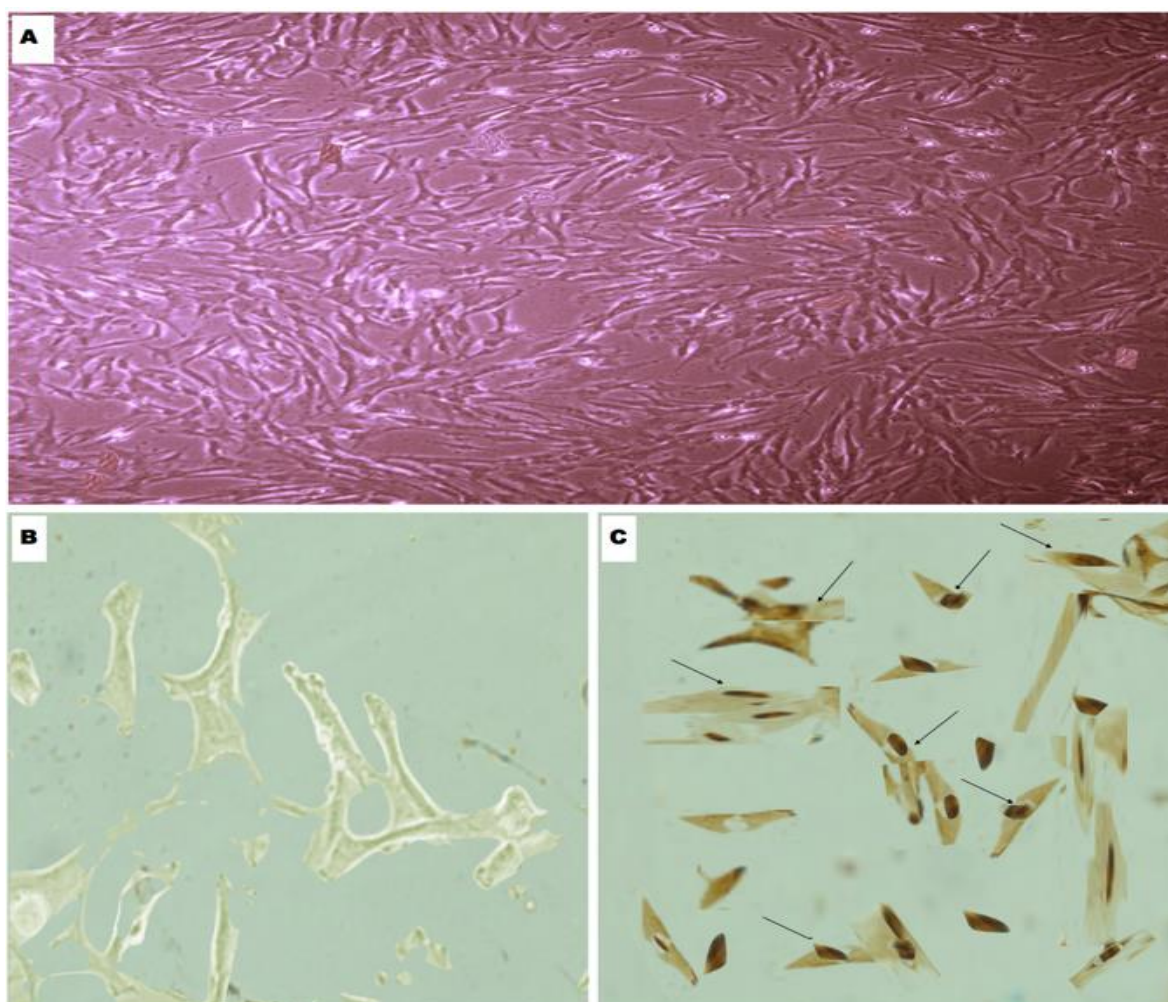


**Figure 1:** Isolation and proliferation of BM-MSCs (40 $\times$ ).

The photomicrograph of cultured BM-MSCs showed their spindle and stellate-shaped appearance with 80% confluence (A). The cell proliferation assay was evaluated via BrdU incorporation of the BM-MSCs for 24 h. BM-MSCs before BrdU staining with no stained nuclei (B). The BrdU

positive cells significantly increased upon reaching the required confluence and the brown-stained nuclei can be seen (C). BM-MSCs: bone marrow-mesenchymal stem cells, BrdU: bromodeoxyuridine.

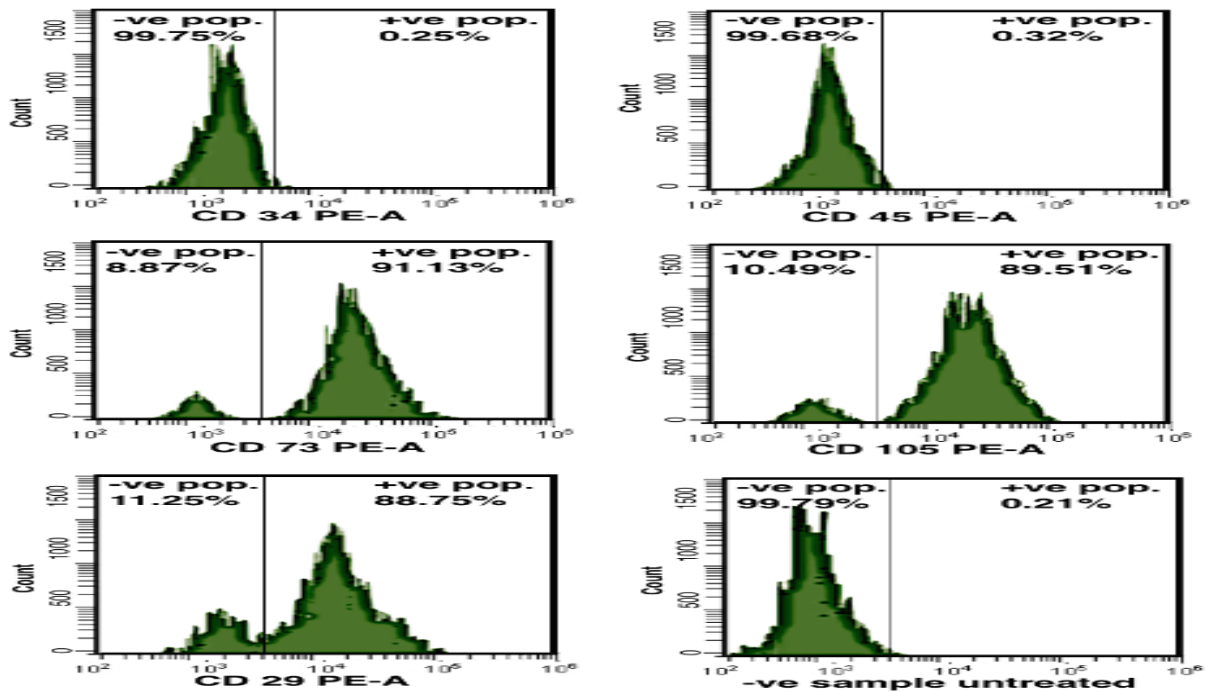


**Figure 2:** Phenotypic analysis.

Cultured BM-MSCs positively expressed CD73 (91.13%), CD105 (89.51%), and CD29 (88.75%), while they negatively expressed CD34 and CD45 antibody staining. The untreated sample resulted in 0.21% +ve population and 99.79% -ve population.

The morphology of the BM-MSCs changed from spindle-shaped to oblate-shaped after differentiation to hepatocyte-like cells (Figure 3). Firstly, the majority of cells exhibited a fibroplastic appearance, with a few cells

being round. The cells were changed from their original cylindrical shape to semi-spindle and spherical-shaped cells on day 7. The majority of cells had a noticeable round appearance with a few cells displaying faint nuclei. From day 14 this cell morphology often changed to more compact oblateness. On day 21 of maturation, polygonal honeycomb-like overloaded cells with hexagonal borders and distinct single or double nuclei were observed and very little intercellular space was seen.

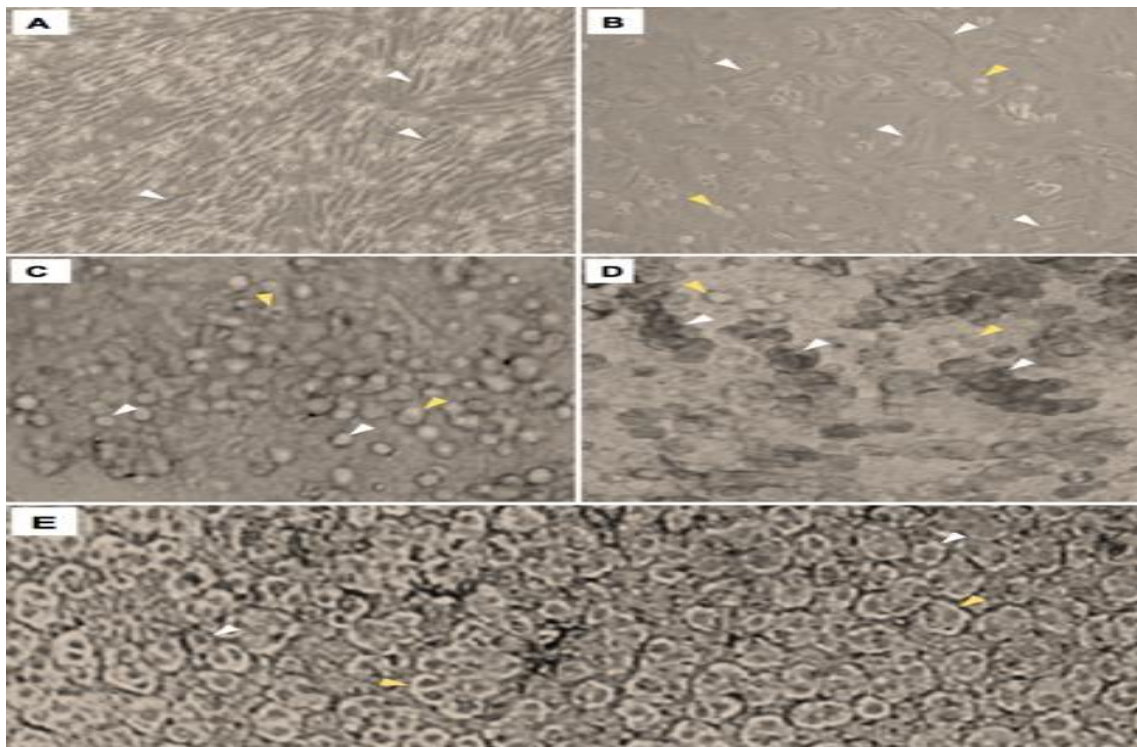


**Figure 3:** Hepatogenic differentiation of BM-MSCs

(A) Day 2, (B) Day 3, (C) Day 7, (D) Day 14, (E) Day 21. (A) On day 2, the morphology of the BM-MSCs had changed from spindle to semi-spindle shape (arrowheads). (B) On day 3, the majority of cells exhibited a fibroplastic appearance (white arrowheads) and a few showed a round appearance (yellow arrowheads). (C) On day 7, the majority of cells were round or spherical-shaped (white arrowheads) with a few cells displaying faint nuclei (yellow arrowheads). (D) By day 14, all cells exhibited a noticeable round appearance with faint nuclei (arrowheads). (E) On day 21, the honeycomb-like overloaded cells can be seen, displaying oblateness with hexagonal borders and having a distinct single nucleus (white arrowheads) or double nuclei (yellow arrowheads) with very little intercellular space. BM-MSCs: bone marrow-mesenchymal stem cells.

Evaluation of the hepatic enzymes ALP, AST, and ALT in the sera of the CCl<sub>4</sub>-induced hepatotoxicity rat model and the effects of silymarin or BM-MSCs or both were used to

evaluate the hepatic status (Table 1). Hepatotoxicity led to alteration in some liver function parameters. Compared with the apparently healthy group, in the CCl<sub>4</sub> hepatotoxicity model, there were significant increases in ALT ( $P < 0.01$ ), AST ( $P < 0.05$ ), ALP ( $P < 0.01$ ), T. Bili ( $P < 0.05$ ), and D. Bili ( $P < 0.05$ ) with a significant decline in albumin ( $P < 0.05$ ) and unchanged total protein or globulin levels. The results revealed that albumin was significantly elevated, and ALT, AST, T. Bili and D. Bili were significantly l ( $P < 0.05$ ) in the silymarin group. The i.v. injection of BM-MSCs significantly restored the activities of ALT, AST, ALP and the T. Bili and D. Bili levels ( $P < 0.05$ ), relative to group of CCl<sub>4</sub> hepatotoxicity rat model. On the other hand, the BM-MSCs + silymarin significantly ameliorated all the biochemical indices and restored them to normal levels by significantly increasing the total protein, globulin and albumin ( $P < 0.05$ ) as well as significantly reducing the levels of ALT ( $P < 0.05$ ), AST ( $P < 0.01$ ), ALP ( $P < 0.05$ ), T. Bili ( $P < 0.05$ ), and D. Bili ( $P < 0.05$ ).

Table 1: Effect of silymarin and/or BM-MSCs on bio-indices and liver enzyme activities in serum of the CCl<sub>4</sub>-induced hepatotoxicity rat model

Parameters	ALT (U/L)	AST (U/L)	ALP (U%)	T. Protein (g%)	Albumin (g%)	Globulin (g%)	T. Bili mg/dl	D. Bili mg/dl
Groups								
Healthy control	82.12 ±3.51	128.76±4.99	117.55 ±5.78	7.83 ±1.22	4.55 ±1.09	3.12 ±0.98	0.45 ±0.02	0.23 ±0.04
CCl <sub>4</sub>	114.65** ±9.54	183.65* ±7.08	163.63** ±854	6.63 ±1.11	3.01* ±0.55	3.31 ±0.88	0.87* ±0.04	0.43* ±0.03
CCl <sub>4</sub> +Silymarin	95.43 <sup>a</sup> ±4.86	131.53 <sup>a</sup> ±3.85	148.73 ±5.82	7.56 ±1.22	3.99 <sup>a</sup> ±0.07	3.43 ±0.23	0.54 <sup>a</sup> ±0.04	0.33 <sup>a</sup> ±0.08
CCl <sub>4</sub> +BM-MSCs	85.65 <sup>a</sup> ±3.65	133.43 <sup>a</sup> ±4.11	129.43 <sup>a</sup> ±5.34	8.83 <sup>a</sup> ±0.88	4.97 <sup>a</sup> ±0.53	4.52 <sup>a</sup> ±0.51	0.51 <sup>a</sup> ±0.03	0.29 <sup>a</sup> ±0.02
CCl <sub>4</sub> +Silymarin+BM-MSCs	82.54 <sup>a</sup> ±6.54	129.65 <sup>b</sup> ±3.54	121.32 <sup>a</sup> ±7.54	8.94 <sup>a</sup> ±0.93	4.65 <sup>a</sup> ±0.76	5.76 <sup>a</sup> ±0.33	0.55 <sup>a</sup> ±0.10	0.21 <sup>a</sup> ±0.04

Means in the same column with \* and \*\* are differ significantly from the healthy control at  $P < 0.05$  and  $P < 0.01$ , respectively. Means in the same column, <sup>a</sup> and <sup>b</sup> are differ significantly from CCl<sub>4</sub> at  $P < 0.05$  and  $P < 0.01$ , respectively.

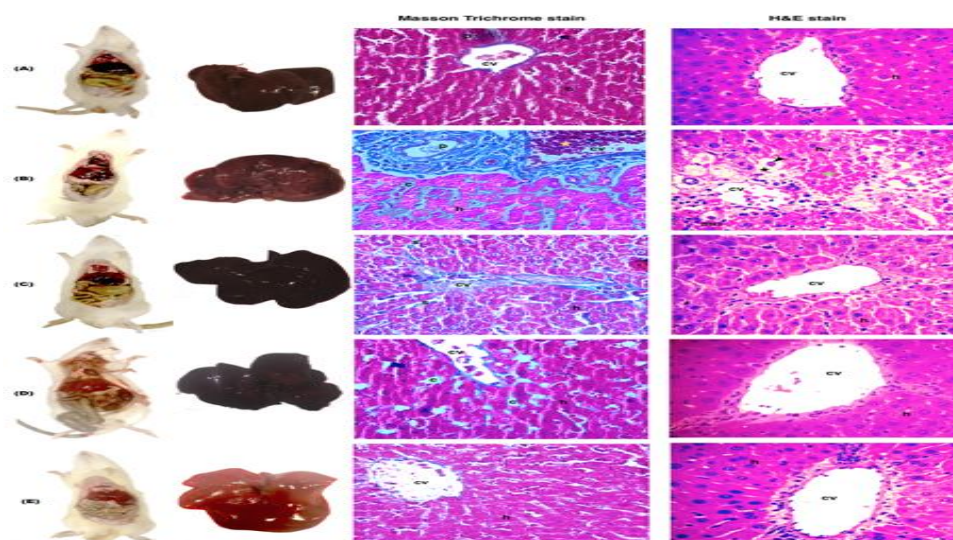


Figure 4: Livers, gross and histological views (400×)

(A) Healthy control, (B) CCl<sub>4</sub>-induced hepatotoxicity model, (C) CCl<sub>4</sub>+silymarin treated, (D) CCl<sub>4</sub>+BM-MSCs treated, (E) CCl<sub>4</sub>+silymarin+BM-MSCs treated. (Scale bar: 40 μm). The gross view of a liver from the healthy control rat group in Figure 4 (A) displays a normal appearance and size. The histological view shows the consistent structure of the liver as a solid organ possessing plates of hepatocytes (h) radiating from the central vein (cv). The stained section shows a typical portal area (p) and slit-like sinusoids (s) lined by endothelial cells (arrowhead). In Figure 4(B), hepatomegaly and a dark, severely congested hepatic surface with fibrotic patches, rough surfaces, and a hard texture are seen in the gross view of the liver of the CCl<sub>4</sub>-induced hepatotoxicity rat model. Histologically, the liver displays abnormal architecture, as seen in the engorgement of the central vein with blood and in the hepatocytes with swollen vacuolated cytoplasm and pyknotic nuclei with collagen fiber (c) deposited between them. Mononuclear cellular infiltration (mn) and erythrocytes are also seen. The liver from the CCl<sub>4</sub> + silymarin group (Figure 4C) is seen anatomically as enlarged and congested with a few fibrotic nodules. Histologically, the liver shows a moderate amount of collagen fiber (c) between the hepatocytes and the obliterated central vein. The liver of the CCl<sub>4</sub>+BM-MSCs group (Figure 4D) macroscopically exhibits a normal size with a dark, congested surface and disappearance of the

fibrotic nodules. Histologically, this liver exhibits a dilated central vein with a few collagen fibers between the hepatocytes. Some hepatocytes display a dark-colored nucleus and acidophilic cytoplasm. The liver from the CCl<sub>4</sub>+ silymarin +BM-MSCs group shown in Figure 4(E) has been restored to a nearly normal appearance, hepatic surface, and size, and the fibrotic nodules and congestion have disappeared. Histologically, the restored architecture of the hepatic lobules can be observed. The hepatocytes are arranged in cords radiating from the central vein and appear with eosinophilic granular cytoplasm and rounded vesicular nuclei. BM-MSCs: bone marrow-mesenchymal stem cells, CCl<sub>4</sub>: carbon tetrachloride.

The antioxidant activities in hepatic tissue were affected in the CCl<sub>4</sub>-induced fibrosis rat model relative to the group of healthy control (Table 2). A significantly increased activity of MDA ( $P < 0.01$ ) and a significantly decreased activities of CAT ( $P < 0.01$ ), SOD, and GSH-Px ( $P < 0.05$ ) were noticed in the CCl<sub>4</sub>-induced fibrosis rat model relative to the normal group. Silymarin administration or BM-MSCs transplantation separately significantly decreased MDA ( $P < 0.01$ ) and increased CAT and SOD ( $P < 0.01$ ). However, compared to the CCl<sub>4</sub>-induced fibrosis rat model, the BM-MSCs + silymarin therapy significantly restored hepatic tissue antioxidant activities by decreasing MDA ( $P < 0.05$ ) and markedly increasing CAT and GSH-Px ( $P < 0.05$ ) activities without changing SOD activity.

Table 2: Effect of silymarin and /or BM-MSCs on hepatic tissue antioxidant enzyme activities of the CCl<sub>4</sub>-induced hepatotoxicity rat model

Parameters	MDA (mol/mg tissue)	CAT (nmol/g tissue)	SOD (U/g tissue)	GPx (U/g tissue)
<b>Groups</b>				
<b>Healthy control</b>	33.45 ±1.65	38.23 ±3.54	9.33 ±2.65	71.87 ±3.76
<b>CCl<sub>4</sub></b>	47.43**±2.56	19.44** ±1.76	5.98* ±1.22	43.65* ±3.65
<b>CCl<sub>4</sub>+Silymarin</b>	25.54 <sup>b</sup> ±2.22	32.98 <sup>b</sup> ±3.76	8.54 <sup>a</sup> ±1.88	48.46 ±4.12
<b>CCl<sub>4</sub>+BM-MSCs</b>	23.20 <sup>b</sup> ±2.05	35.16 <sup>b</sup> ±2.51	8.98 <sup>a</sup> ±1.32	52.54 ±4.33
<b>CCl<sub>4</sub>+Silymarin+BM-MSCs</b>	34.65 <sup>a</sup> ±3.88	29.54 <sup>a</sup> ±2.93	7.65 ±2.87	70.54 <sup>a</sup> ±3.16

Means in the same column with \* and\*\* are differ significantly from the healthy control at  $P < 0.05$  and  $P < 0.01$ , respectively. Means in the same column, <sup>a</sup> and <sup>b</sup> are differ significantly from CCl<sub>4</sub> at  $P < 0.05$  and  $P < 0.01$ , respectively.

TNF-α, IL-4, IL-10, and IL-17 serum levels in all the studied groups of rats are presented in Table 3. The CCl<sub>4</sub>-induced hepatotoxicity was associated with an elevated level of pro-inflammatory cytokine; TNF-α ( $P < 0.05$ ) and a

decrease in anti-inflammatory cytokines; IL-4, IL-10, and IL-17 ( $P < 0.05$ ) relating to the normal healthy rats. Otherwise, the level of IL-17 raised significantly ( $P < 0.05$ ) and TNF-α significantly reduced in the rats treated with silymarin ( $P < 0.05$ ). Treatment with BM-MSCs or both silymarin and BM-MSCs restored the cytokine levels, as confirmed by a significant reduction in TNF-α serum level and a significant rise in the IL-4, IL-10, and IL-17 levels ( $P < 0.05$ ).

Table 3: Effect of silymarin and /or BM-MSCs on serum cytokine concentration (ng/mL) of the CCl<sub>4</sub>-induced hepatotoxicity rat model

Parameters	TNF-α (ng/ml)	IL-4 (ng/ml)	IL-10 (ng/ml)	IL-17 (ng/ml)
<b>Groups</b>				
<b>Healthy control</b>	9.87 ±1.94	11.87 ±1.22	9.66 ±1.67	14.65 ±1.32
<b>CCl<sub>4</sub></b>	16.43* ±1.04	7.96* ±1.11	5.65* ±1.54	9.54* ±1.02
<b>CCl<sub>4</sub>+Silymarin</b>	10.76 <sup>a</sup> ±1.44	11.99 ±2.08	7.31 ±1.54	13.98 <sup>a</sup> ±1.22
<b>CCl<sub>4</sub>+BM-MSCs</b>	10.54 <sup>a</sup> ±1.45	11.55 <sup>a</sup> ±1.33	9.31 <sup>a</sup> ±1.33	14.08 <sup>a</sup> ±1.32
<b>CCl<sub>4</sub>+Silymarin+BM-MSCs</b>	10.43 <sup>a</sup> ±1.55	10.95 <sup>a</sup> ±1.35	10.11 <sup>a</sup> ±1.54	15.91 <sup>a</sup> ±1.29

Means in the same column with \* and\*\* are differ significantly from the healthy control at  $P < 0.05$  and  $P < 0.01$ , respectively. Means in the same column, <sup>a</sup> and <sup>b</sup> are differ significantly from CCl<sub>4</sub> at  $P < 0.05$  and  $P < 0.01$ , respectively.

The expression of Akt and p-Akt proteins was evaluated by Western blot. Bands of Akt were expressed in the liver protein of all experimental groups (Figure 5). Bands of p-

Akt were more visible in the CCl<sub>4</sub>-induced hepatotoxicity and CCl<sub>4</sub> + silymarin groups than in the other groups. Densitometric measurements were performed of the Akt and p-Akt band intensities using IMAGEJ software with β-actin as the control. The highest p-Akt band intensity was found in the CCl<sub>4</sub>-induced hepatotoxicity group, which indicated Akt phosphorylation (Figure 6).

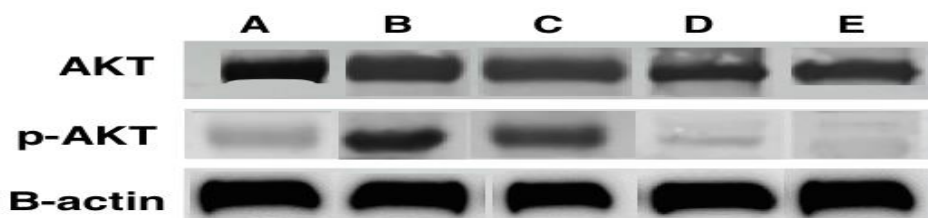


**Figure 5:** Total Akt and p-Akt protein expression in different experimental groups (Western blot)

(A) healthy control group, (B) CCl<sub>4</sub> group, (C) CCl<sub>4</sub>+silymarin group, (D) CCl<sub>4</sub>+BM-MSCs group, (E) CCl<sub>4</sub>+silymarin+BM-MSCs group. (Loading control - immunoreactivity to β—actin).

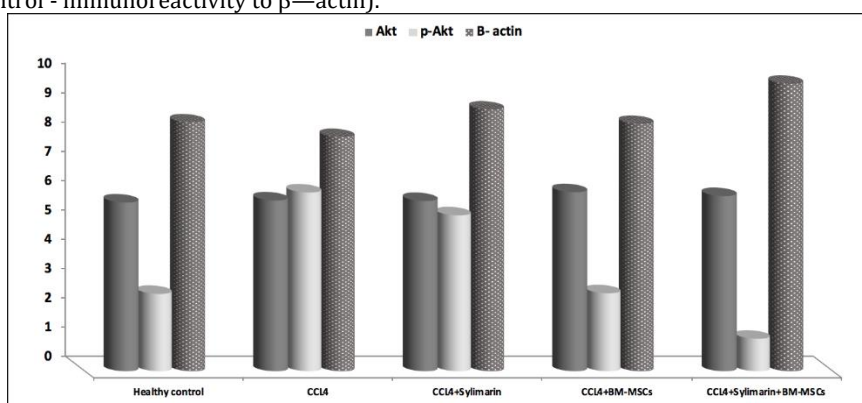


**Figure 6:** Densitometric measures of band intensity for Akt and p-Akt using IMAGEJ software. BM-MSCs: bone marrow-mesenchymal stem cells, CCl<sub>4</sub>: carbon tetrachloride.

## DISCUSSION

The topic of liver damage control is continually being discussed, with the hope of finding the ideal method for amelioration. Although cell therapy was established for liver damage management, there is disagreement regarding the outcome. Incompetence in the treatment of fibrosis has been reported by some authors [28]. Various factors, such as timing and dose, can interfere with the results. Previously, BM-MSC transplantation has been shown to result in maintenance of fibrogenesis via the stimulation of HSC and myofibroblasts [29]. Similar results were obtained in a cirrhotic liver mouse model [30] and immunocompromised mice [31] treated with MSCs. The homing of stem cells to the liver and differentiating to myofibroblasts has been previously reported [32]. Therefore, in the present study, BM-MSCs were transplanted alone or in combination with silymarin to a CCl<sub>4</sub>-induced hepatotoxicity rat model. The isolated BM-MSCs can be provoked for hepatocyte-like cells differentiation by some growth factors, as previously discussed [33]. The properties of the BM-MSCs isolated in the present work via phenotyping to viability and proliferation are similar to those of the cells in a previous study [34].

Various laboratory models have been used in the past. The CCl<sub>4</sub>-induced hepatotoxicity rat model was chosen due to its similarity to human hepatotoxicity [Jiménez *et al.*,

1992]. The solvent CCl<sub>4</sub> is widely used in the chemical industry and its hepatic and renal toxic activity is widely known. As a potential environmental contaminant, it provides a means for volatile chemicals contacting and absorption. In the present study, the CCl<sub>4</sub>-induced hepatotoxicity rat model showed a significant decrease in albumin levels accompanied by a significant rise in ALT, AST, and ALP, compared to the apparently healthy group. The significant decrease in albumin may have been due to decreased synthesis by the dysfunctional liver or to dehydration resulting from diarrhea caused by the CCl<sub>4</sub> treatment [35]. Previous studies have reported CCl<sub>4</sub>-induced steatosis, fibrosis, cirrhosis [36], and eventually cell death [37] and lipid peroxidation [4]. Normally, liver transaminases are found and synthesized inside the cell [AST in the mitochondria and ALT inside the cytoplasm]. The toxicity has led to leakage of enzymes into the blood [27] and CCl<sub>4</sub> treatment resulted in an increase of serum ALP with high levels of direct and indirect Bili [38]. These parameters indicated cholestasis and pathological variation of biliary flux [39].

In the present study, we used two well-known management applications: silymarin as a standard hepatoprotective drug and BM-MSCs as a cell-based therapy. The oral injection dose and duration of the silymarin treatment were parallel to those of Abdel Salam *et al.* [40]. However, Abenavoli *et al.* [41] used silymarin

for a short time of five days and at a low dose of 50 mg/kg, while Onalan *et al.* [42] used 300 mg/kg/day for seven days. The results revealed a significant elevation in albumin and a significant reduction in ALT, AST, T. Bili and D. Bili in the silymarin group. The i.v. injection of BM-MSCs significantly restored the activities of ALT, AST, ALP, T. Bili and D. Bili levels compared to the CCl<sub>4</sub> hepatotoxicity rat model group. On the other hand, the BM-MSCs + silymarin significantly ameliorated all the biochemical indices and restored them to normal levels by significantly increasing the total protein, globulin, and albumin as well as significantly reducing the ALT, AST, ALP, T. Bili, and D. Bili the hepatoprotective effect of silymarin has been discussed earlier [43]. Silymarin has the ability to suppress enzyme leakage and to maintain the integrity of the plasma membrane, hence, preventing liver damage. The potential of silymarin to treat fibrotic rat liver has been previously reported [44] and was attributed to the anti-fibrotic activity of the silymarin. In addition, it has been used to repair damaged hepatocytes [45]. The mechanism was previously attributed to the elevation of protein biosynthesis by the ribosomal RNA [46] and was confirmed by liver function tests [Mohamed *et al.*, 2016]. Concerning BM-MSC treatment and hepatic damage, Zhang *et al.* [1] reported that the cell-based therapy was begun as a new and effective strategy to repair liver damage. The obtained data were in parallel with the work of Leibacher *et al.* [15], who demonstrated the beneficial effects of MSCs on the regeneration of damaged tissue, reduction of inflammation and oxidative stress, and modulation of immune reactions.

The antioxidant activities in hepatic tissue were affected in the CCl<sub>4</sub>-induced hepatotoxicity rat model relative to the healthy control group. MDA activity significantly increased along with a significant decline in CAT, SOD, and GPx. The data were in parallel with previously recorded findings [47]. Individual separate administration of silymarin or BM-MSCs significantly reduced MDA and increased CAT and SOD. However, compared to the CCl<sub>4</sub>-induced hepatotoxicity rat model, the BM-MSCs + silymarin therapy significantly restored hepatic tissue antioxidant activities by decreasing MDA and markedly increasing CAT and GPX activities without changing SOD activity. These antioxidants and immunomodulation features were suggested in an earlier study [48]. It is common knowledge that oxidative stress is caused by the exhaustion of antioxidant enzyme activity in response to reactive oxygen species [ROS]. An elevated MDA is commonly used as a biomarker of lipid peroxidation [49]. The positive support of silymarin in the oxidant/antioxidant balance has been investigated previously [25] and results confirmed that silymarin defensive effects may be at least partially concerning to its antioxidant activity [11, 50].

CCL<sub>4</sub> induced hepatotoxicity was associated with increased pro-inflammatory cytokines; TNF- $\alpha$  and reduced anti-inflammatory cytokines; IL-4, IL-10 and IL-17 relative to the healthy control group. Furthermore, a significant increase in the level of IL-17 and significant decrease of TNF- $\alpha$  were reported in rats treated with silymarin. BM-MSCs therapy or both silymarin and BM-MSCs combination restored the cytokines levels as indicated by a significantly reduced TNF- $\alpha$  serum level and significantly raised IL-4, IL-10 and IL-17 levels. This data was parallel to the previously recorded [51]. It was known the involvement of IFN- $\gamma$  in the pathogenesis of liver fibrosis [52]. On the contrary, IL-4, IL-10 and IL-17 were previously considered as anti-fibrotic cytokines and their

elevation indicated shifting cytokines from anti-inflammatory to pro-fibrotic condition [52]. Several experimental investigations have explored that IL-17 signaling of fibrogenesis and the production of pro-fibrotic cytokine in liver [Meng *et al.*, 2012]. Treatment with BM-MSCs increased serum level of IL-10 and decreased Th17 which reduced HSC activation and collagen deposition [53].

Upon histopathological examination, the liver slides stained by H & E and MTC revealed a regular structure in the healthy control group. Those of the CCl<sub>4</sub>-treated group displayed abnormal architecture, including engorgement of the central vein with blood, swollen vacuolated cytoplasm and pyknotic nuclei in the hepatocytes, and collagen fiber deposition between the cells. Mononuclear cellular infiltration and erythrocytes were also observed. The CCl<sub>4</sub> + silymarin-treated group showed moderate collagen fiber deposition and an obliterated central vein. The CCl<sub>4</sub> + BM-MSCs-treated group showed a dilated central vein with a small amount of collagen between the hepatocytes. The CCl<sub>4</sub> + silymarin + BM-MSCs-treated group exhibited remodeling of hepatic lobules construction. The hepatocytes were aligned in cords radiating from the central vein and displayed eosinophilic granular cytoplasm and rounded vesicular nuclei.

The Akt and p-Akt expression was evaluated in the present study via Western blot. Bands of p-Akt were much more prominent in the CCl<sub>4</sub>-induced hepatotoxicity group than in the other groups, indicating a higher phosphorylation of the Akt signal accompanied by higher collagen levels in the liver tissue. Densitometric measurement of the band intensities was performed for Akt and p-Akt using IMAGEJ software with  $\beta$ -actin as the control. The p-Akt band intensity was higher in CCl<sub>4</sub> group than the various other groups. This result was in parallel with the work of Wang *et al.* [26]. The collagen that was formed was believed to have originated in the hepatic stellate cells [54]. These data further supported the findings of earlier biochemical work [55].

These data suggest that the BM-MSCs with silymarin had a synergistic effect via an antioxidant defense mechanism in attenuating or alleviating oxidative stress in the CCl<sub>4</sub>-induced hepatotoxicity rat model. The combination succeeded in eliminating histopathological alterations. The findings of the current investigation prove the usefulness of BM-MSCs and their synergism with silymarin in providing a significant hepatoprotective effect against hepatotoxicity induced by CCl<sub>4</sub>.

## CONCLUSION

In light of the results of the present study, treatment using a combination of BM-MSCs and silymarin could protect the liver from hepatotoxicity by inhibiting collagen deposition and improving liver enzyme and antioxidant activity. Furthermore, the results were supported by the Akt/p-Akt signaling cascade via down-regulation of Akt phosphorylation.

## AUTHOR CONTRIBUTIONS

TIA and AAZ collaborated in the study design. AAZ and FAMA planned the experiments. FAMA isolated BM-MSCs and completed their proliferation, characterization and hepatogenic differentiation. TSA, YMA and SMA shared in BM-MSCs characterization. FAMA, YMA and SMA carried out the biochemical, histological and immunological studies. AAZ and FAMA interpreted the results, made the write up and statistically analyzed the data and made

illustrations. All authors have read and approved the final manuscript.

#### ACKNOWLEDGEMENT

Grateful and thankfulness for the Qassim University Deanship of Scientific Research for providing financial support for this study through Project Number 3432-cavm-2018-1-14-S.

#### POTENTIAL CONFLICT OF INTEREST

The data and research results are honest, and the authors have no conflicting financial interest.

#### REFERENCES

1. Zhang JJ, Meng X, Li Y, Zhou Y, Xu DP, Li S, Li HB. Effects of melatonin on liver injuries and diseases. *Int J Mol Sci* 2017; Apr,18(4):673.
2. Khalifa YH, Mourad GM, Stephanos WM, Omar SA, Mehanna RA. Bone Marrow-Derived Mesenchymal Stem Cell Potential Regression of Dysplasia Associating Experimental Liver Fibrosis in Albino Rats. *BioMed Res Int* 2019; Nov,6,2019.
3. Wang H, Naghavi M, Allen C, Barber RM, Bhutta ZA, Carter A, Casey DC, Charlson FJ, Chen AZ, Coates MM, Coggeshall M. Global, regional, and national life expectancy, all-cause mortality, and cause-specific mortality for 249 causes of death, 1980–2015: a systematic analysis for the Global Burden of Disease Study 2015. *The lancet* 2016; Oct 8,388(10053):1459-544.
4. Luo XY, Meng XJ, Cao DC, Wang W, Zhou K, Li L, Guo M, Wang P. Transplantation of bone marrow mesenchymal stromal cells attenuates liver fibrosis in mice by regulating macrophage subtypes. *Stem Cell Res Ther* 2019; Dec,10(1):1-1.
5. Polo ML, Riggio M, May M, Rodríguez MJ, Perrone MC, Stallings-Mann M, Lanari C. Activation of PI3K/Akt/mTOR signaling in the tumor stroma drives endocrine therapy-dependent breast tumor regression. *Oncotarg* 2015;6(26):22081.
6. Akbar DH, Kawther AH. Nonalcoholic fatty liver disease in Saudi type 2 diabetic subjects attending a medical outpatient clinic: prevalence and general characteristics. *Diabetes care* 2003; Dec,26(12):3351-2.
7. Al-Nozha MM, Al-Mazrou YY, Al-Maatouq MA, Arafah MR, Khalil MZ, Khan NB, *et al.* Obesity in Saudi Arabia. *Saudi Med J* 2005; 26:824-9.
8. Al-Johani JJ, Aljehani SM, Alzahrani GS. Assessment of Knowledge about Liver Cirrhosis among Saudi Population. *The Egyptian Journal of Hospital Med* 2018;71(2),2443-2446.
9. Volarevic V, Nurkovic J, Arsenijevic N, Stojkovic M. Concise review: therapeutic potential of mesenchymal stem cells for the treatment of acute liver failure and cirrhosis. *Stem cells* 2014; Nov,32(11):2818-23.
10. Ferrer JR, Chochechanachaisakul A, Wertheim JA. New tools in experimental cellular therapy for the treatment of liver diseases. *Curr transplant reports* 2015; Jun,2(2):202-10.
11. Onalan AK, Tuncal S, Kilicoglu S, Celepli S, Durak E, Kilicoglu B, Devrim E, Barlas AM, Kismet K. Effect of silymarin on oxidative stress and liver histopathology in experimental obstructive jaundice model. *Acta chirurg brasil* 2016; Dec,31(12):801-6.
12. Vargas-Mendoza N, Madrigal-Santillán E, Morales-González Á, Esquivel-Soto J, Esquivel-Chirino C, y González-Rubio MG, Gayosso-de-Lucio JA, Morales-González JA. Hepatoprotective effect of silymarin. *World j hepatol* 2014; Mar,6(3):144.
13. Abenavoli L, Capasso R, Milic N, Capasso F. Milk thistle in liver diseases: past, present, future. *Phytother Res* 2010; Oct,24(10):1423-32.
14. Hu C, Li L. Improvement of mesenchymal stromal cells and their derivatives for treating acute liver failure. *J Mol Med* 2019; Jun,13:1-20.
15. Leibacher J, Henschler R. Biodistribution, migration and homing of systemically applied mesenchymal stem/stromal cells. *Stem Cell Res Ther* 2016; Dec,7(1):7.
16. Tsukamoto H, Matsuoka M, French SW. Experimental models of hepatic fibrosis: a review. In *Seminliv dis* 1990; Feb,10(1):56-65.
17. Jobling M. National, Research Council (NRC) Nutrient requirements of poultry. 9th Rev. Ed. National Academy Press. Washington, DC. USA 1994.
18. Abo-Aziza FA, Zaki AK, El-Maaty AM. Bone marrow-derived mesenchymal stem cell (BM-MSC): a tool of cell therapy in hydatid experimentally infected rats. *Cell Reg* 2019; Dec,8(2):58-71.
19. Lee SH, Cha SH, Kim CL, Lillehoj HS, Song JY, Lee KW. Enhanced adipogenic differentiation of bovine bone marrow-derived mesenchymal stem cells. *J App Anim Res* 2015; Jan,2,43(1):15-21.
20. Abo-Aziza FA, Zaki AA, Amer AS, Lotfy RA. Dihydrotestosterone and 17-Estradiol Enhancement of in vitro Osteogenic Differentiation of Castrated Male Rat Bone Marrow Mesenchymal Stem Cells (rBMMSCs). *Int j hematol oncol stem cell res* 2019; Oct,13(4):208.
21. Yamaza T, Fatima SA, Ratih Y *et al.* In vivo hepatogenic capacity and therapeutic potential of stem cells from human exfoliated deciduous teeth in liver fibrosis in mice. *Stem Cell Res Ther* 2015; 6:171.
22. Al-Mutairi KS, Tariq IA, Zaki AA. Osteogenic/Adipogenic Differentiation of Intact and Ovariectomized Young and Adult Female Rat Bone Marrow Mesenchymal Stem Cells (BMMSC). *RJPBCS* 2019;10(2):253-65.
23. Akiyama K, You YO, Yamaza T, Chen C, Tang L, Jin Y, Chen XD, Gronthos S, Shi S. Characterization of bone marrow derived mesenchymal stem cells in suspension. *Stem cell res ther* 2012; Dec,3(5):40.
24. Ye D, Li T, Heraud P, Parnpai R. Effect of chromatin-re modeling agents in hepatic differentiation of rat bone marrow-derived mesenchymal stem cells in vitro and in vivo. *Stem Cells Int* 2016; Jan,1;2016.
25. Yilmaz İ, Hatipoglu HS, Taslidere E, Karaaslan M. Comparing the regenerative effects of Silymarin and Apricot on liver regeneration after partial hepatectomy in rats. *Biomedical Res* 2018;29(7),1465-1473.
26. Wang R, Song F, Li S, Wu B, GuY, Yuan Y. Salvianolic acid A attenuates CCl4-induced liver fibrosis by regulating the PI3K/AKT/mTOR, Bcl-2/Bax and caspase-3/cleaved caspase-3 signaling pathways. *Drug Des Dev Ther* 2019;13,1889.
27. Mohamed EE, Husien Husien S, Osama Abdulla FA, Engy RF. Studies on Hepatoprotective Effect of Pentoxifylline on Ccl4 Induced Liver Fibrosis in Guinea Pigs. *Int Clin Pathol J* 2015;1(4):00021.

28. Mannheimer EG, Quintanilha LF, Carvalho AB, Paredes BD, Gonçalves de Carvalho F, Takyia CM, Resende CM, Ferreira da Motta Rezende G, Carlos Campos de Carvalho A, Schanaider A, Coeli dos Santos Goldenberg R. Bone marrow cells obtained from cirrhotic rats do not improve function or reduce fibrosis in a chronic liver disease model. *Clin transplant* 2011; Jan,25(1):54-60.
29. Haldar D, Henderson NC, Hirschfield G, Newsome PN. Mesenchymal stromal cells and liver fibrosis: a complicated relationship. *The FASEB J* 2016; Dec,30(12):3905-28.
30. Russo FP, Alison MR, Bigger BW, Amofah E, Florou A, Amin F, Bou-Gharios G, Jeffery R, Iredale JP, Forbes SJ. The bone marrow functionally contributes to liver fibrosis. *Gastroenterol* 2006; May,130(6):1807-21.
31. Di Bonzo LV, Ferrero I, Cravanzola C, Mareschi K, Rustichell D, Novo E, Sanavio F, Cannito S, Zamara E, Bertero M, Davit A. Human mesenchymal stem cells as a two-edged sword in hepatic regenerative medicine: engraftment and hepatocyte differentiation versus profibrogenic potential. *Gut* 2008; Feb,57(2):223-31.
32. Li C, Kong Y, Wang H, Wang S, Yu H, Liu X, Yang L, Jiang X, Li L, Li L. Homing of bone marrow mesenchymal stem cells mediated by sphingosine 1-phosphate contributes to liver fibrosis. *J hepatology*. 2009; Jun,50(6):1174-83.
33. Al Ghrbawy NM, Afify RA, Dyaa N, El Sayed AA. Differentiation of bone marrow: derived mesenchymal stem cells into hepatocyte-like cells. *Ind J Hematol Bl Transfus* 2016; Sep32(3), 276-83.
34. Zaki AA, Almundarij TI, Abo-Aziza FA. Comparative characterization and osteogenic/adipogenic differentiation of mesenchymal stem cells derived from male rat hair follicles and bone marrow. *Cell Reg* 2020;9(1), 1-14.
35. El-Gazzar UB, El-Far AH. The ameliorative effect of Phoenix dactylifera extract on CCl4 hepatotoxicity in New Zealand rabbits. *J App Sci Res* 2009; Sep,1082-7.
36. Khalil MR, El-Demerdash RS, Elminshawy HH, Mehanna ET, Mesbah NM, Abo-Elmatty DM. Therapeutic effect of bone marrow mesenchymal stem cells in a rat model of carbon tetrachloride induced liver fibrosis. *Biomed J* 2020; May7.
37. Amin A, Mahmoud-Ghoneim D. Texture analysis of liver fibrosis microscopic images: a study on the effect of biomarkers. *Acta Biochim Biophys Sin*. 2011; Mar,43(3):193-203.
38. Domitrović R, Jakovac H, Milin Č, Radošević-Stašić B. Dose-and time-dependent effects of luteolin on carbon tetrachloride-induced hepatotoxicity in mice. *Exper Toxicol Pathol* 2009;61(6):581-589.
39. Lalitsingh R, Bhatt J, Patel J. Hepatoprotective activity of ethanolic extracts of bark of *Zanthoxylum armatum* DC in CCl4 induced hepatic damage in rats. *J ethnopharmacol* 2010; Feb,127(3):777-80.
40. Abdel-Salam OM, Sleem AA, El-Mosallamy AE, Shaffie N. Effect of Echinacea alone or in combination with silymarin in the carbon-tetrachloride model of hepatotoxicity. *Compar Clin Pathol* 2012; Dec,21(6):1483-92.
41. Abenavoli L, Capasso R, Milic N, Capasso F. Milk thistle in liver diseases: past, present, future. *Phytother Res* 2010; Oct,24(10):1423-32.
42. Onalan AK, Tuncal S, Kilicoglu S, Celepli S, Durak E, Kilicoglu B, Devrim E, Barlas AM, Kismet K. Effect of silymarin on oxidative stress and liver histopathology in experimental obstructive jaundice model. *Acta chirurg brasil* 2016; Dec,31(12):801-6.
43. Vargas-Mendoza N, Madrigal-Santillán E, Morales-González Á, Esquivel-Soto J, Esquivel-Chirino C, y González-Rubio MG, Gayosso-de-Lucio JA, Morales-González JA. Hepatoprotective effect of silymarin. *World j hepatol* 2014;6(3), 144.
44. Al-Rasheed N, Faddah L, Sharaf IA, Mohamed AM, Al-Rasheed N, Abdelbaky N. Assessment of the potential role of silymarin alone or in combination with Vitamin E and/or curcumin on the carbon tetrachloride induced liver injury in rat. *Brazil Arch Biol Technol* 2015; Dec,58(6):833-42.
45. Cetinkunar S, Tokgoz S, Bilgin BC, Erdem H, Aktimur R, Can S, Erol HS, Isgoren A, Sozen S, Polat Y. The effect of silymarin on hepatic regeneration after partial hepatectomy: is silymarin effective in hepatic regeneration? *Int j clin exper med* 2015;8(2):2578.
46. Feher J, Lengyel G. Silymarin in the prevention and treatment of liver diseases and primary liver cancer. *Curr pharm biotechnol* 2012; Jan,13(1):210-7.
47. Aithal AP, Laxminarayana KB, Raviraja NS, Kumar N. Therapeutic Potential of Human Bone Marrow Derived Mesenchymal Stromal Cells in Combination with Silymarin against Carbon Tetrachloride Induced Liver Cirrhosis in Wistar Rats. *JKIMSU* 2017;6(4).
48. Volarevic V, Nurkovic J, Arsenijevic N and Stojkovic M. Concise review: Therapeutic potential of mesenchymal stem cells for the treatment of acute liver failure and cirrhosis. *Stem Cells* 2014; 32:2818-2823.
49. Yao XM, Zhao J, Li Y, Li Y. Effects of bicyclol on liver regeneration after partial hepatectomy in rats. *Digests dis sci*. 2009; Apr,54(4):774-81.
50. Jung YS, Kim SJ, Kim YS, Choi DW, Kim YC. Alterations in sulfur amino acid metabolism in mice treated with silymarin: a novel mechanism of its action involved in enhancement of the antioxidant defense in liver. *Planta med* 2013; Aug,79(12):997-1002.
51. De Souza VC, Pereira TA, Teixeira VW, Carvalho H, de Castro MC, D'assunção CG, de Barros AF, Carvalho CL, de Lorena VM, Costa VM, Teixeira AA. Bone marrow-derived monocyte infusion improves hepatic fibrosis by decreasing osteopontin, TGF-β1, IL-13 and oxidative stress. *World J Gastroenterol* 2017; Jul,23(28):5146.
52. Pinheiro D, Leirós L, Dáu JB, Stumbo AC, Thole AA, Cortez EA, Mandarim-de-Lacerda CA, Carvalho LD, Carvalho SN. Cytokines, hepatic cell profiling and cell interactions during bone marrow cell therapy for liver fibrosis in cholestatic mice. *PloS one* 2017; Nov,12(11): e0187970.
53. Milosavljevic N, Gazdic M, Simovic Markovic B, Arsenijevic A, Nurkovic J, Dolicanin Z, Jovicic N, Jetic I, Djonov V, Arsenijevic N, Lukic ML. Mesenchymal stem cells attenuate liver fibrosis by suppressing Th17 cells—an experimental study. *Transpl int* 2018; Jan,31(1):102-15.
54. Wang H, Naghavi M, Allen C, Barber RM, Bhutta ZA, Carter A, Casey DC, Charlson FJ, Chen AZ, Coates MM, Coggeshall M. Global, regional, and national life expectancy, all-cause mortality, and cause-specific mortality for 249 causes of death, 1980–2015: a

systematic analysis for the Global Burden of Disease Study 2015. *The Lancet*. 2016; Oct,388(10053):1459-544.

55. Mohamed HE, Elswefy SE, Rashed LA, Younis NN, Shaheen MA, Ghanim AM. Bone marrow-derived mesenchymal stem cells effectively regenerate fibrotic liver in bile duct ligation rat model. *Exper Biol Med* 2016; Mar,241(6):581-91.
56. Papanas N, Pafili K, Demetriou M, Chatzikosma G, Papachristou S, Papazoglou D. Automated Measurement of Sural Nerve Conduction is a Useful Screening Tool for Peripheral Neuropathy in Type 1 Diabetes Mellitus. *The Review of Diabetic Studies*. 2019;15(1).